Radiology Case Reports 19 (2024) 6141–6146

Available online at www.sciencedirect.com

ScienceDirect

journal homepage: www.elsevier.com/locate/radcr

Case Report

Parotid gland MALT lymphoma with amyloid deposition, challenges in preoperative diagnosis: A case report ☆

Yuriko Watanabe, MD[a], Hiroyuki Fujii, MD, PhD[a,], Saki Yamamoto, MD[a], Sota Masuoka, MD[a], Ryoma Kobayashi, MD[a], Nana Fujii, MD[a], Akihiro Nakamata, MD[a], Takeharu Kanazawa, MD, PhD[b], Mitsuru Matsuki, MD, PhD[c], Harushi Mori, MD, PhD[a]*

[a] *Department of Radiology, Jichi Medical University, Tochigi, Japan*
[b] *Department of Otolaryngology-Head and Neck Surgery, Jichi Medical University, Tochigi, Japan*
[c] *Department of Pediatric Radiology, Jichi Children's Medical Center, Tochigi, Japan*

ARTICLE INFO

Article history:
Received 23 August 2024
Revised 13 September 2024
Accepted 16 September 2024

Keywords:
MALT lymphoma
Amyloidosis
MRI
Sjögren syndrome
Parotid gland

ABSTRACT

Mucosa-associated lymphoid tissue (MALT) lymphoma commonly arises from chronic inflammation or autoimmune diseases, such as Sjögren syndrome (SjS). Although rare, amyloid deposition in MALT lymphoma has been reported. We present a rare case of parotid gland MALT lymphoma in a 49-year-old woman, in whom preoperative diagnosis was challenging due to atypical imaging findings resulting from amyloid deposits. MRI showed T2-hypointense and T1-iso- to slightly hyperintense masses in the left parotid gland and right sublingual gland, with predominant marginal contrast enhancement and no significant diffusion restriction. Additionally, atrophy and fatty replacement of the parenchyma were noted in bilateral parotid glands, suggesting SjS. Left superficial parotidectomy was performed and pathological findings confirmed MALT lymphoma with extensive amyloid deposition. Histopathological findings of the resected parotid gland parenchyma also suggested SjS. MALT lymphoma should be considered in the differential diagnosis of multiple salivary gland masses in patients with suspected SjS. If MRI reveals atypical imaging findings for malignant lymphoma, particularly T2-hypointensity with no significant diffusion restriction, the possibility of amyloid deposition in MALT lymphoma should be considered.

Abbreviations: MALT, mucosa-associated lymphoid tissue; SjS, Sjögren syndrome; WBC, white blood cell; RBC, red blood cell; MRI, magnetic resonance imaging; T2WI, T2-weighted image; T1WI, T1-weighted image; DWI, diffusion-weighted image; ADC, apparent diffusion coefficient; DFS, direct fast scarlet; FDG-PET, fluorodeoxyglucose-positron emission tomography; SUVmax, maximum standardized uptake value; CT, computed tomography; FLC, free light chain; HE, hematoxylin-eosin.

☆ Competing Interests: The authors declare that they have no known competing financial interests or personal relationships that could have appeared to influence the work reported in this paper.

* Corresponding author.
E-mail address: hiroyuki.fujii@jichi.ac.jp (H. Fujii).

https://doi.org/10.1016/j.radcr.2024.09.083

Introduction

Mucosa-associated lymphoid tissue (MALT) lymphoma is a subtype of extranodal marginal zone B-cell lymphoma that arises from mucosa-associated lymphoid tissue, including the gastrointestinal tract, lung, oropharynx, salivary gland, ocular adnexa, and skin. It often arises in the setting of chronic inflammation or autoimmune disease, such as Sjögren syndrome (SjS) [1]. Although rare, amyloid deposition in MALT lymphoma has been reported at various sites, including the stomach, lungs, and ocular adnexa [2]. Amyloid deposition in MALT lymphoma of the salivary glands has also been reported, but its detailed imaging findings have not been described in the literature. Herein, we present a case of parotid gland MALT lymphoma with extensive amyloid deposition, where preoperative diagnosis was challenging due to atypical imaging findings resulting from amyloid deposits, and discuss its imaging findings.

Case report

A 49-year-old woman presented to our hospital with a 5-year history of progressively increasing left subauricular masses. The patient had a history of surgery for uterine cervical cancer 14 years earlier. Physical examination revealed firm, nontender left subauricular mass. Laboratory blood test evaluations showed a white blood cell (WBC) count of 2800/μL, and a red blood cell (RBC) count of $3.55 \times 10^6/\mu$L, indicating a mild decrease in both these parameters. Other physical examinations and laboratory findings were unremarkable.

Ultrasonography showed multiple, round, hypoechoic masses up to 2 cm in diameter, with punctate calcifications in bilateral parotid glands. Color Doppler imaging showed no significant blood flow signals within the hypoechoic masses. The bilateral submandibular glands showed heterogeneous echotexture with scattered small hypoechoic lesions, suggesting chronic salivary gland inflammation.

Magnetic resonance imaging (MRI) showed well-defined masses in the left parotid gland and the right sublingual gland (Fig. 1). The masses revealed hypointensity on T2-weighted images (T2WI) and iso- to slight hyperintensity on T1-weighted images (T1WI). Diffusion-weighted imaging (DWI) (b = 1000 s/mm^2) and the apparent diffusion coefficient (ADC) map did not show significant diffusion restriction (Figs. 1A, B, D, E). Gadolinium-enhanced fat-suppressed T1WI showed enhancement at the margins and faint enhancement at the center of the mass (Figs. 1C and F). Additionally, atrophy and fatty replacement of the parenchyma were noted in bilateral parotid glands, suggesting SjS. Given the pres-

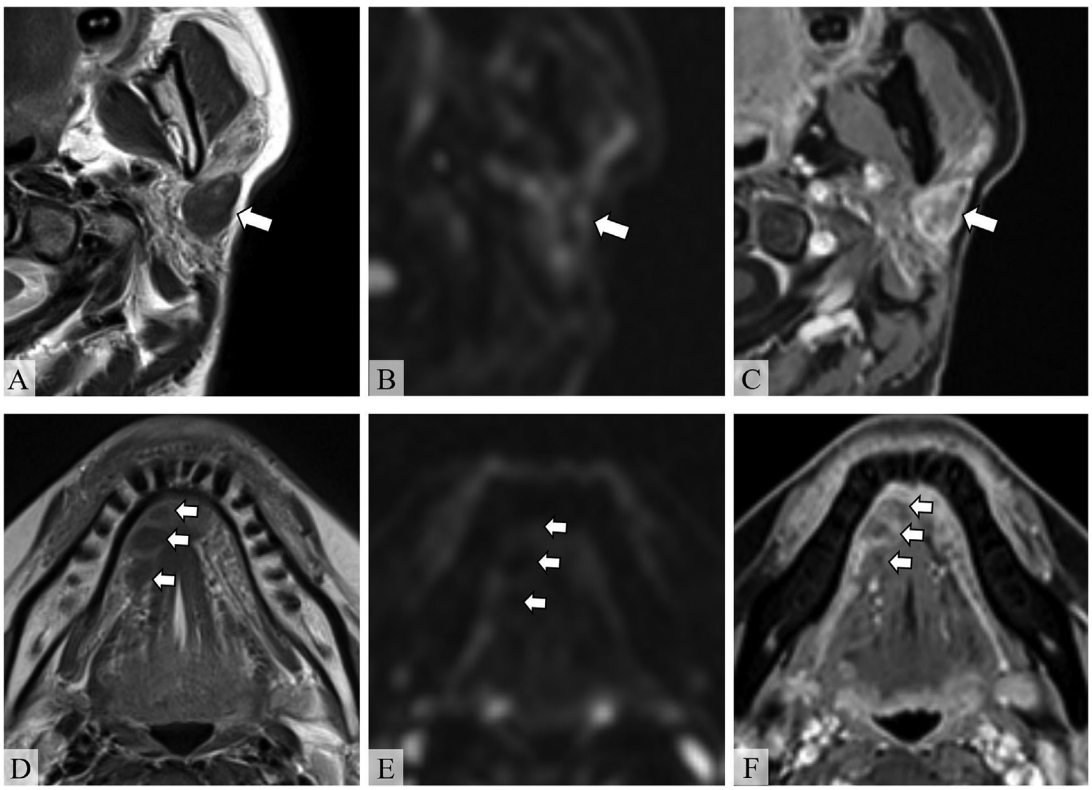

Fig. 1 – MRI of the head and neck. (A, D) Axial T2-weighted images (T2WI), (B, E) axial diffusion-weighted images (DWI) (b = 1000 s/mm^2), and (C, F) axial gadolinium-enhanced fat-suppressed T1WI (Gd-FS-T1WI). Well-defined T2-hypointense masses are observed in the left parotid gland and right sublingual gland (A, D, arrows). The masses do not show hyperintensity on DWI, indicating no diffusion restriction (B, E, arrows). Gd-FS-T1WI shows enhancement at the margins and faint enhancement at the center of the mass (C, F, arrows). Atrophy and fatty replacement of the parenchyma is noted in the left parotid gland, suggesting Sjögren syndrome.

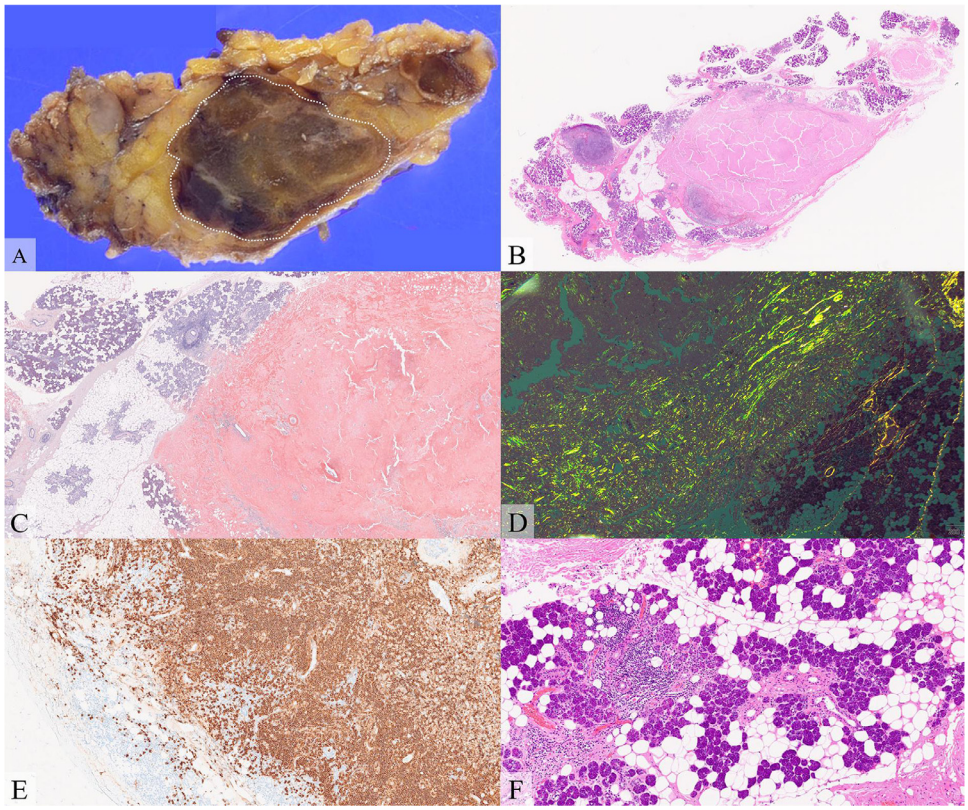

Fig. 2 – Histopathological and immunohistological findings. (A) Formalin-fixed specimen, (B) hematoxylin-eosin (HE) staining, (C) direct fast scarlet (DFS) staining, (D) DFS staining under cross-polarized light, (E) CD20 antibody staining, and (F) HE staining.
Gross pathology shows a brownish mass in the resected parotid gland (A, dashed oval). Microscopically, the mass consists of eosinophilic, hyalinized, amorphous material. The eosinophilic amorphous material is positive for DFS staining and shows green birefringence under polarized light microscopy, suggesting amyloid deposits. Lymphocytes and plasma cells at the periphery of the amyloid deposits are positive for CD20 (E). The resected parotid tissue shows stromal fibrosis and fatty replacement, and lymphocytic infiltration around the exocrine glands, suggesting Sjögren syndrome (F).

ence of multiple salivary gland nodules in a patient with suspected SjS, MALT lymphoma was considered. However, MRI showed T2-hypointensity with no significant diffusion restriction, which was atypical imaging findings for malignant lymphoma. Other than MALT lymphoma, cellular type pleomorphic adenoma, Warthin tumor, oncocytoma, malignant salivary gland tumors, IgG4-related disease, and amyloidosis were considered in the differential diagnosis for T2-hypointense salivary gland lesions.

The patient underwent left superficial parotidectomy for definitive diagnosis because the mass showed a tendency to increase in size. Macroscopically, a brownish ovoid mass, measuring 2.5 × 1.6 × 1.1 cm, was seen within the resected left parotid gland (Fig. 2A). Microscopically, the mass mainly consisted of amyloid deposits, confirmed by direct fast scarlet (DFS) staining and green birefringence under polarized light microscopy (Figs. 2B-D). Lymphocytes and plasma cells, which were positive for CD20, C79a, and Bcl-2 staining, and negative for Bcl-6, CD10, and CyclinD1 staining, were observed at the periphery of the amyloid deposits, consistent with MALT lymphoma (Fig. 2E). The resected parotid tissue showed stromal fibrosis and fatty replacement, with lymphocytic infiltration around the exocrine glands (Fig. 2F). In addition, serum SS-A antibody and antinuclear antibodies were positive, strongly suggesting SjS.

Postoperatively, to evaluate for systemic involvement of MALT lymphoma, 18F-Fluorodeoxyglucose-positron emission tomography (FDG-PET) scan was performed, which revealed multiple anterior mediastinal masses with a maximum standardized uptake value (SUVmax) of 2.72 (Fig. 3A). Chest computed tomography (CT) showed punctate calcification within the masses (Fig. 3B). On MRI, the masses showed marked hypointensity on T2WI with no restricted diffusion, similar to the salivary gland masses (Figs. 3C and D). Thoracoscopic biopsy of the anterior mediastinal mass indicated the presence of amyloid deposition; however, the presence of MALT lymphoma in the specimen was not confirmed.

Biopsies of the skin, bone marrow, stomach, duodenum, and rectum, performed to exclude systemic amyloidosis, showed no evidence of amyloid deposition. Laboratory tests showed that serum immunoglobulin free light chain (FLC) kappa and lambda levels were not elevated, with an FLC ratio of 1.17. Urine M-protein was negative. Additionally, since the patient had no clinical symptoms suggesting systemic amy-

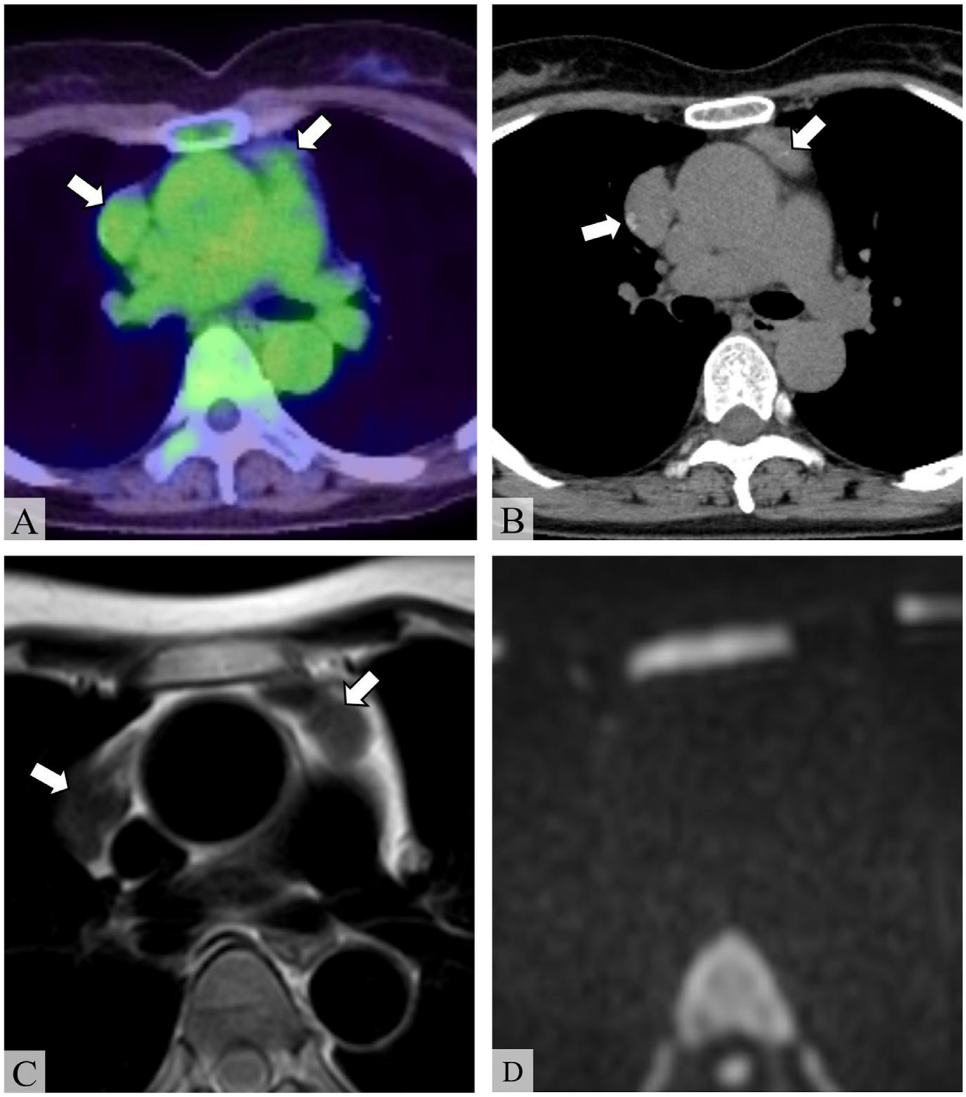

Fig. 3 – Imaging findings of the anterior mediastinal masses. (A) 18F-Fluorodeoxyglucose-positron emission tomography (FDG-PET), (B) unenhanced chest computed tomography (CT), (C) axial T2-weighted image (T2WI), and (D) axial diffusion-weighted image (DWI) (b = 1000 s/mm^2). FDG-PET shows multiple anterior mediastinal masses with a maximum standardized uptake value (SUVmax) of 2.72 (A, arrows). Unenhanced CT shows calcification within the masses (B, arrows). The masses show homogeneous hypointensity on T2WI and do not show hyperintensity on DWI, indicating no diffusion restriction (C, D, arrows).

loidosis, systemic amyloidosis was clinically excluded. Ultimately, the salivary glands and anterior mediastinal masses were considered to represent a series of MALT lymphomas with extensive amyloid deposition. Since the patient was asymptomatic, a watchful waiting approach was adopted. Over 1 year of watchful waiting, the patient has remained asymptomatic without tumor progression.

Discussion

MALT lymphoma is composed of small B cells that most typically include marginal zone cells, accounting for 7%-8% of non-Hodgkin B cell lymphoma [3]. The stomach is the most common site of MALT lymphomas and frequent extragastric sites include the salivary glands, skin, orbits and conjunctiva, lung, thyroid gland, upper airways, breast, other gastrointestinal sites, and the liver [2]. Among salivary glands, the parotid gland is the most commonly affected site (78%), with 8.5% of cases involving bilateral parotid glands [4].

SjS is a well-known autoimmune disease that increases the risk of developing MALT lymphoma, particularly in the salivary glands. In the present case, MRI showed atrophy and fatty replacement of the bilateral parotid glands, and both serum SS-A antibodies and antinuclear antibodies were positive. Furthermore, histopathological findings of the resected parotid gland revealed stromal fibrosis, fatty replacement, and lymphocytic infiltration around the exocrine glands, consistent with SjS. Although lip biopsy of the minor salivary glands, the

gold standard for diagnosis of SjS, was not performed in the present case, parotid biopsy has been reported to have comparable diagnostic capabilities [5]. The findings in the present case strongly suggested the diagnosis of SjS, which might have contributed to the high-risk status for the development of MALT lymphoma.

Amyloid deposition in MALT lymphoma is thought to originate from immunoglobulin light chains produced by neoplastic plasmacytoid cells. Although rare, it has been reported at various sites, including the stomach, salivary glands, lungs, ocular adnexa, etc [2,4,6]. Among the salivary glands, amyloid deposition has been reported in the parotid gland, submandibular gland, and minor salivary glands [2,7–9]. It has been reported that amyloid deposits in MALT lymphoma are often extensive relative to the tumor area. In a pathological study of 20 MALT cases with amyloid deposition, the area of amyloid deposits was greater than that of lymphoma in 60% of cases [2]. Additionally, in 35% of the cases, amyloid deposits occupied more than 90% of the total area. In that report, the lymphomatous component was typically present as a peripheral rim around the amyloid nodule or in dense bands or foci throughout the mass [2]. In the present case, MALT lymphoma of the left parotid gland was mostly replaced by amyloid deposits, and the lymphomatous component was observed at the periphery of the amyloid deposits. The absence of systemic amyloidosis suggests that immunoglobulin light chains produced in MALT lymphoma were insufficient in quantity or in amyloidogenic properties to give rise to amyloid deposits beyond their region of local production. The other salivary gland masses and mediastinal masses were also speculated as being part of a series of MALT lymphoma with amyloid deposition, although biopsy of the mediastinal masses showed only amyloid deposits. A previous study reported that only amyloid deposits were detected in 1 biopsy specimen, while lymphomas were detected in other biopsy specimens [2]. This suggests that sampling artifacts might play a significant role in underdiagnosing amyloid-associated lymphoma. Another case series also reported a case in which only amyloid deposits were found [10]. The authors speculated that the MALT lymphoma regressed and only amyloid deposits remained in that case.

On imaging, salivary gland MALT lymphoma typically presents as a diffuse or solid mass, often with internal cystic components and calcification [11]. The solid component typically shows mild to moderate hypointensity on T1WI, and iso- or mild hyperintensity on T2WI, with low ADC values (mean 0.64×10^{-3} mm^2/s, range $0.48\text{-}0.82 \times 10^{-3}$ mm^2/s) [12]. Contrast-enhanced MRI shows homogeneous, mild to moderate enhancement and a rapid-increase and gradual pattern on dynamic contrast-enhanced imaging [12,13]. On 18F-FDG-PET, the reported SUVmax for MALT lymphomas of the parotid gland is 7.7 ± 3.7 [14]. In contrast, MR imaging findings of amyloid deposits have shown that both T1WI and T2WI show variable signal intensity [15]. Contrast-enhanced T1WI typically shows either faint or intense enhancement [16]. These variabilities are considered as being due to the site of deposition and the degree of amyloid protein accumulation [17]. Hypointensity on T2WI is thought to represent dense amyloid protein deposits [15]. In the present case, the parotid gland MALT lymphoma with amyloid deposition showed atypical imaging findings: hypointensity on T2WI and iso- to slight hyperintensity on T1WI, with no significant diffusion restriction. Contrast enhancement at the margins and faint enhancement in the center of the mass were considered to correspond to MALT lymphoma at the margins and extensive amyloid deposits, respectively.

As in the present case, amyloid deposition alters the typical imaging findings of MALT lymphoma, making preoperative diagnosis challenging. Our experience suggests that MALT lymphoma should be considered in the differential diagnosis when multiple salivary gland masses are encountered in patients with suspected SjS. If MRI reveals atypical imaging findings for malignant lymphoma, particularly T2-hypointensity with no significant diffusion restriction, the possibility of amyloid deposition in MALT lymphoma should be considered.

Conclusion

We described a case of parotid gland MALT lymphoma with extensive amyloid deposition. The amyloid deposition significantly altered the typical imaging findings of MALT lymphoma, complicating the preoperative diagnosis. Radiologists should consider the possibility of amyloid deposition in suspected cases of MALT lymphoma when MRI reveals atypical imaging findings, particularly T2-hypointensity with no diffusion restriction.

Patient consent

Written informed consent was obtained from the patient for publication of this case report.

REFERENCES

[1] Zucca E, Bertoni F. The spectrum of MALT lymphoma at different sites: biological and therapeutic relevance. Blood 2016;127(17):2082–92.
[2] Ryan RJH, Sloan JM, Collins AB, Mansouri J, Raje NS, Zukerberg LR, et al. Extranodal marginal zone lymphoma of mucosa-associated lymphoid tissue with amyloid deposition. Am J Clin Pathol 2012;137(1):51–64.
[3] WHO Classification of Tumours Editorial Board WHO classification of tumours. 5th ed. Lyon: International Agency for Research on Cancer; 2020.
[4] Jackson AE, Mian M, Kalpadakis C, Pangalis GA, Stathis A, Porro E, et al. Extranodal marginal zone lymphoma of mucosa-associated lymphoid tissue of the salivary glands: a multicenter, international experience of 248 patients (IELSG 41). Oncologist 2015;20(10):1149–53.
[5] Spijkervet FKL, Haacke E, Kroese FGM, Bootsma H, Vissink A. Parotid gland biopsy, the alternative way to diagnose sjögren syndrome. Rheum Dis Clin North Am 2016;42(3):485–99.
[6] Zhang Q, Pocrnich C, Kurian A, Hahn AF, Howlett C, Shepherd J, et al. Amyloid deposition in extranodal marginal zone lymphoma of mucosa-associated lymphoid tissue: a clinicopathologic study of 5 cases. Pathol Res Pract 2016;212(3):185–9.

[7] Gabali A, Ross CW, Edwards PC, Schnitzer B, Danciu TE. Pediatric extranodal marginal zone B-cell lymphoma presenting as amyloidosis in minor salivary glands: a case report and review of the literature. J Pediatr Hematol Oncol 2013;35(3):e130–3.
[8] Perera E, Revington P, Sheffield E. Low grade marginal zone B-cell lymphoma presenting as local amyloidosis in a submandibular salivary gland. Int J Oral Maxillofac Surg 2010;39(11):1136–8.
[9] Kojima M, Sugihara S, Iijima M, Ono T, Yoshizumi T, Masawa N. Marginal zone B-cell lymphoma of minor salivary gland representing tumor-forming amyloidosis of the oral cavity. A case report. J Oral Pathol Med 2006;35(5):314–16.
[10] Arai H, Tajiri M, Kikunishi N, Nakamura S, Inafuku K, Ishikawa Y, et al. A spectrum of Thymic mucosa-associated lymphoid tissue lymphoma and Thymic amyloidosis in the patient with Auto immune disease: a case series. Mediastinum 2021;5:12.
[11] Zhu L, Wang P, Yang J, Yu Q. Non-Hodgkin lymphoma involving the parotid gland: CT and MR imaging findings. Dentomaxillofacial Radiol 2013;42(9):20130046.
[12] Kato H, Kanematsu M, Goto H, Mizuta K, Aoki M, Kuze B, et al. Mucosa-associated lymphoid tissue lymphoma of the salivary glands: MR imaging findings including diffusion-weighted imaging. Eur J Radiol 2012;81(4):e612–7.
[13] Zhu L, Zhang C, Hua Y, Yang J, Yu Q, Tao X, et al. Dynamic contrast-enhanced MR in the diagnosis of lymphoassociated benign and malignant lesions in the parotid gland. Dentomaxillofacial Radiol 2016;45(4):20150343.
[14] Qi S, Huang MY, Yang Y, Schöder H, Teckie S, Noy A, et al. Uptake of [18F]fluorodeoxyglucose in initial positron-emission tomography predicts survival in MALT lymphoma. Blood Adv 2018;2(6):649–55.
[15] Ogilvie J, Zhao R, Camelo-Piragua S, Ibrahim M, Lobo R, Kim J. Magnetic resonance imaging of a temporal lobe cerebral amyloidoma. Radiol Case Rep 2022;17(8):2820–3.
[16] Gandhi D, Wee R, Goyal M. CT and MR imaging of intracerebral amyloidoma: case report and review of the literature. AJNR Am J Neuroradiol 2003;24(3):519–22.
[17] Lee J, Krol G, Rosenblum M. Primary amyloidoma of the brain: CT and MR presentation. AJNR Am J Neuroradiol 1995;16(4):712–14.